Available online at www.sciencedirect.com
ScienceDirect
Surface Science 601 (2007) 1536–1543
SURFACE SCIENCE
www.elsevier.com/locate/susc

Experimental confirmation of the EPES sampling depth paradox for overlayer/substrate systems

M. Vos *, M.R. Went

Atomic and Molecular Physics Laboratories, Research School of Physical Sciences and Engineering, The Australian National University, Canberra 0200, Australia

Received 27 October 2006; accepted for publication 12 January 2007
Available online 19 January 2007

Abstract

Elastic-peak electron spectroscopy (EPES) has been one of the main tools for obtaining the inelastic mean free path of electrons in solids. Recently it has become clear that, if this type of experiment is done using an energetic electron beam (20–40 keV) and large scattering angles, then the recoil energies of the elastic scattering event for different elements can be resolved. This recoil energy is mass dependent and this fact makes it possible to separate the elastic-peak contributions due to electrons scattered from light and heavy elements. Here we use this energy separation to determine experimentally the sampling depth for an overlayer/substrate system. The sampling depth for a (high-Z) Au overlayer on a (low-Z) C substrate is found to be about two orders of magnitude smaller than for a C overlayer on a Au substrate, whereas the inelastic mean free path of electrons in both materials differ much less. This effect is shown to be a consequence the strong Z dependence of the elastic scattering cross section. The dependence of the spectra on the electron kinetic energy and sample rotation is also dramatically different for both sample geometries.

Keywords: Thin films; Elastic electron scattering

1. Introduction

Elastic scattering of electrons from surfaces is used in electron spectroscopy [1–3] and microscopy [4]. In electron spectroscopy the intensity of the elastic peak is used to determine the inelastic mean free path (IMFP), and this technique is referred to as EPES (elastic-peak electron spectroscopy) [5]. In microscopy the strong dependence of the elastic-scattering cross section on the atomic number Z is the basis of the contrast in images obtained from the intensity of backscattered electrons in scanning electron microscopy. In these applications it is tacitly assumed that elastic scattering does not change the energy of the energetic electrons.

Large-angle elastic scattering of energetic electrons from an atom implies a significant momentum transfer from the electron to an atom. The atom acquiring this momentum will necessarily also acquire kinetic energy. Hence the kinetic energy of the scattered electron is reduced by this amount. Thus the energy of the reflected electron depends on the mass of the atom it scattered from. This energy loss was first demonstrated by Boersch some 40 years ago [6], and in recent years this small energy loss can be routinely resolved in state-of-the-art spectrometers [7–9].

If electrons with an energy of 1–3 keV are used it is hard to separate the contributions of different elements completely, except for the case of hydrogen [10,11]. Using 30 keV electrons and a scattering angle of 45° it was possible to resolve the contribution of carbon from the contribution of germanium and it was also shown that these measurements provide information about the sample geometry [12]. Using a peak fitting procedure the area of the Ge peak relative to that of the C peak could be determined. The observed intensity ratio was a strong function of measurement geometry, as a consequence of changing

* Corresponding author.
E-mail address: maarten.vos@anu.edu.au (M. Vos).

0039-6028/$ - see front matter © 2007 Elsevier B.V. All rights reserved.
doi:10.1016/j.susc.2007.01.014

inelastic energy-loss probabilities. Thus this technique can be used to study inelastic energy loss processes if the sample composition/morphology is known, or vise versa, the sample composition/morphology can be studied if estimates of the mean free path are available. Encouraged by these results we optimized our spectrometer for this type of measurement by increasing the electron beam energy to 40 keV and adding an electron gun, for which the scattering angle is 120°. Now peaks of heavy and light elements are completely separated and peak areas can be determined with little ambiguity due to the fitting procedure. This method resembles in many way Rutherford backscattering (RBS) as is done at MeV energies using ions, and hence we often refer to these experiments as electron Rutherford backscattering (ERBS) experiments.

These developments have made many new experiments feasible. As a first example we want to show here that, for suitable samples, we can determine the information depth (ID) in EPES experiments performed at high energies for overlayer-substrate systems. The concept of ID was introduced by Jablonski and Powell [13] and is defined as the thickness of the surface layer from which a certain fraction of the signal (we use 95% in this work) originates. Until now Monte Carlo simulations were the only way to obtain an estimate of the ID. For homogenous materials it was found that the information depth is of the order of the mean free path. Hence it came somewhat as a surprise that computer simulations indicated that for overlayer-substrate systems the information depth can be greatly reduced (high Z overlayer on a low Z substrate, the ID of this system can be much shorter than the ID of the overlayer material and the ID of the substrate material) [14] or increased (low Z overlayer on a high Z substrate, the ID of this system can be much larger than the ID of both the overlayer material and the ID of the substrate material) [15]. This effect is especially pronounced at high energies. The strong Z dependence of the elastic-scattering cross section was pinpointed as the cause of this effect, but is was assumed that these result could not be verified experimentally.

We will show that we can separate the elastic-scattering contribution of the overlayer and substrate, and hence we can ascertain for which overlayer thickness 95% of the elastic peak originates from the overlayer. Thus for those samples and measurement conditions the ID is equal to the overlayer thickness. We can monitor the overlayer/substrate intensity ratio as a function of geometry and incoming energy. This gives even more insight into the processes determining the ratio. We will see that the two cases (heavy overlayer on a light substrate and light overlayer on a heavy substrate) react very differently to changes in energy and geometry.

2. Background

If an incoming electron with momentum $\boldsymbol{p}_0$ scatters from an atom with mass M over an angle θ, then the magnitude of the momentum transfer $\boldsymbol{q}$ to this atom is given by (see e.g. [8]):

$$q = 2p_0 \sin(\theta/2). \tag{1}$$

If the atom was stationary before the collision, it obtains a kinetic energy (recoil energy) of $q^2/2M$. The energy of the electron is reduced by this amount. Generally the atoms are not stationary before the collision, due to thermal vibrations, and even at 0 K we have zero-point motion. If the atom had a momentum $\boldsymbol{k}$ *before* the collision, then the recoil energy is given by the difference in kinetic energy of the atom before and after the collision:

$$E_r = \frac{(\mathbf{k}+\mathbf{q})^2}{2M} - \frac{k^2}{2M} = \frac{q^2}{2M} + \frac{\mathbf{q}\cdot\mathbf{k}}{M}. \tag{2}$$

The first term of the final result determines the average recoil energy and the second term describes the Doppler broadening of this peak. Thus (besides the energy resolution of the experiment) the width of the elastic peak is determined by the momentum distribution of the atoms. In the harmonic approximation, there is a simple connection between peak width (standard deviation σ) and mean kinetic energy of the atoms [16]:

$$\sigma = \sqrt{\frac{4}{3}\overline{E_k}\,\overline{E_r}} \tag{3}$$

with $\overline{E_k}$ the average kinetic energy of the atom and $\overline{E_r}$ the mean recoil energy, i.e. $q^2/2M$. $\overline{E_r}$ is determined by the experimental condition (kinetic energy of the beam and scattering angle). $\overline{E_k}$ is a target property, it changes with sample temperature, and can be calculated from the phonon spectrum. Until recently experimental determination of $\overline{E_k}$ was restricted to deep-inelastic neutron scattering (see e.g. [16]). The large overlap between these neutron scattering experiments and the current electron scattering experiment is discussed in [17].

Two elements can only be resolved if their recoil energy E_r differs by more than the experimental resolution and the intrinsic peak width at that momentum transfer. This means that large energies (10's of keV) and large scattering angles are required. In the present experiment the energy was varied from 20 keV to 40 keV, and the scattering angle was 120°. These high energies imply large mean free paths and the combination of large energies and large scattering angle means that the elastic-scattering cross sections are small indeed. An overview of these quantities is given in Table 1. The values given in this table are based on theory (elastic differential cross section) or extrapolation (aided by theory) of values calculated for lower energies to much higher ones (IMFP). Thus the quoted IMFP values should be considered not much more than an educated guess.

At these energies the elastic-scattering cross section is relatively large at very small ($\simeq$1°) angles but decreases sharply with increasing scattering angle. We assume that, just as in ion RBS, these experiments can be interpreted in a single-scattering approximation. Multiple scattering will happen, but will, in almost all cases, be the combination

Table 1
Calculated mean recoil energy ($\overline{E_r}$), inelastic mean free path λ (using the TPP-2M formula [18]) and differential elastic-scattering cross section at 120° (as obtained from the ELSEPA package [20]), for C and Au at the indicated primary energies. For carbon a recent publication [19] gives rather different values for λ. These are given as well

E_0 (keV)	$\overline{E_r}$ Au (eV)	$\overline{E_r}$ C (eV)	λ_C (Å) [18]	λ_C (Å) [19]	λ_{Au} (Å) [18]	$\frac{d\sigma}{d\Omega}$ C (cm^2)	$\frac{d\sigma}{d\Omega}$ Au (cm^2)
20	0.17	2.80	347	220	135	2.0E−22	6.1E−20
25	0.21	3.51	421	268	164	1.3E−22	4.1E−20
30	0.26	4.23	494	315	192	9.0E−23	3.0E−20
40	0.35	5.70	637	405	247	5.0E−23	1.8E−20

of a small-angle scattering event (≃1°) and a large-angle scattering event (≃120° for our geometry). The large-angle scattering event occurs at the maximum depth of the trajectory and determines the recoil energy. Thus the single-scattering approximation is valid if the influence of the small-angle scattering event on the trajectory and the recoil energy can be neglected. Hence for now we will interpret our experiment in a single-scattering approximation, but we will point out later that there is some justification in the experimental results for this approximation. An investigation, probably using Monte Carlo simulation, into the level of accuracy that can obtained at these energies within a single-scattering approximation would be desirable. A closely related problem was discussed in the context of transport theory by Dwyer [21]. He found that single-scattering theory gave reasonable answers for $E > 2$ keV and $Z < 47$. This suggests that the single scattering theory should work well for all Z at $E > 20$ keV.

Consider first a homogeneous system. Within the single-scattering approximation the probability $P(\lambda, z)$ that an electron reaches the analyzer without energy loss after scattering at depth z is simply given by

$$P(\lambda, z) = e^{-z/(\lambda \cos\theta_{in})} e^{-z/(\lambda \cos\theta_{out})} \quad (4)$$

with λ the IMFP and θ_{in}, θ_{out} the angle of the incoming and outgoing trajectory with respect to the surface normal. The count rate (I) for the total elastic peak of a thick homogeneous system is then per unit current:

$$I = C \int_0^\infty N \frac{d\sigma}{d\Omega} P(\lambda, z) dz = CN \frac{d\sigma}{d\Omega} \lambda \frac{\cos\theta_{in} \cos\theta_{out}}{\cos\theta_{in} + \cos\theta_{out}} \quad (5)$$

with C a constant describing the spectrometer opening angle, detection efficiency, etc., N the number of atoms per unit volume, and $\frac{d\sigma}{d\Omega}$ the differential elastic cross section for the scattering angle selected by the spectrometer. Assuming that $\frac{d\sigma}{d\Omega}$ and N are known, then, by comparing the count rate for two different materials, we can obtain the ratio of their IMFPs. Without the single-scattering approximation, we have to invoke the help of e.g. Monte Carlo simulations to obtain this ratio, and this is how the IMFP is usually obtained in EPES.

For a two-layer system, with thickness of the overlayer t, we obtain for the count rate of electrons scattered in the overlayer:

$$I_o(t) = C \int_0^t N_o \left(\frac{d\sigma}{d\Omega}\right)_o P(\lambda_o, z) dz, \quad (6)$$

where the subscript o refers to the properties of the overlayer. The count rate of the substrate (subscript s) is given by

$$I_s(t) = CN_s P(\lambda_o, t) \left(\frac{d\sigma}{d\Omega}\right)_s \lambda_s \frac{\cos\theta_{in} \cos\theta_{out}}{\cos\theta_{in} + \cos\theta_{out}} \quad (7)$$

and this is just the count rate of the substrate without overlayer, multiplied by the probability that the electron does *not* lose energy in the overlayer.

The information depth ID is defined as the thickness of the surface layer within which a large majority (95%) of the trajectories are contained. Thus, the ID for a homogeneous system is the thickness t for which the intensity as calculated by Eq. (6) is 95% of the intensity for a layer of infinite thickness (Eq. (5)). For our spectrometer, when we choose $\theta_{in} = \theta_{out} = 45°$, the ID is given by 1.06λ.

For an overlayer system there is not such a general relation. From Table 1 it is clear that for the Au–C system the $\frac{d\sigma}{d\Omega}$ values of C and Au vary by about 300. As we will see this large variation in cross section has a huge effect on the probing depth.

3. Experiment

The experiments were done with the Electron Momentum Spectrometer of the Australian National University. This spectrometer is described extensively elsewhere [22]. In the case of elastic-scattering experiments an electron gun emits a 500 eV electron beam. The analyzers operate at a pass energy of 200 eV, and the analyzers are floating at −300 V in order to measure the elastic peak. The sample and its surroundings are at a potential of +19.5–39.5 kV. Hence electrons are scattered from the sample with an energy between 20 and 40 keV. In order to assure that the elastic peak can be measured with good resolution the combined drift and ripple of the −300 (analyzer) and −500 V (filament) power supplies should be less than 100 meV. Drift and ripple of the 19.5–39.5 kV power supply can be much larger than this value, without affecting the outcome of the measurement.

The Electron Momentum Spectrometer has a gun at ≃45° relative to the analyzer. Although this scattering angle was sufficient to show e.g. that the elastic signal of C/Ge was composed of two peaks, it is clear from Eqs. (1) and (2) that a larger peak separation would be obtained if a larger scattering angle could be employed. Hence we equipped the

spectrometer with an additional gun (Kimball Physics ELG-2 with a barium oxide cathode for low thermal spread of the beam). The actual geometry is sketched in Fig. 1. Both analyzer and gun are on a cone with half-angle of approximate 45°. The gun is in the vertical plane through the axis of the cone. The analyzer in the horizontal plane. The corresponding scattering angle is 120°. This larger scattering angle increases the recoil energy by about a factor of 5, but at the same energy the cross section goes down by a factor of approximately 25.

The sample can be rotated around the vertical axis, and this angle is called α. For $\alpha = 0°$ the surface normal of the sample is along the axis of the cone (and $\theta_{in} = \theta_{out} = 45°$). For $\alpha = 45°$ the sample normal would be pointing towards the analyzer ($\theta_{in} = 60°$, $\theta_{out} = 0°$).

Two samples were prepared. Both samples used arc-evaporated carbon foils supplied by Arizona Film company. These foils are sp^2 bonded films, graphitic of nature with little long-range order. The carbon film was floated off a microscope slide and picked up on a shim. One sample was a carbon foil with an areal density of 32.0 μg/cm^2, using the density of graphite this corresponds to a thickness of 1400 Å. This foil was mounted on a stainless steel shim on which we deposited Au *in situ*. At these high energies we are not very sensitive to surface impurities. The elastic peak of the carbon film was measured before Au deposition. There was some excess intensity at the high-energy side of the peak, at an energy loss range corresponding to atomic masses between Na and Fe. No excess intensity was observed for the small energy loss values corresponding to Au. The intensity of the impurity signal was less than 5% of the carbon signal, as judged from imperfections in the fit of the C elastic peak. As the elastic scattering cross section increases roughly with Z^2 this means that the impurity concentration was less than 1%. Au was subsequently deposited on C by evaporation. The thickness of the Au film was measured using a crystal thickness monitor. Most likely the evaporated Au atoms will not form a smooth layer on carbon but small clusters (islands). As long as the cluster size is much smaller than the IMFP of Au this detail will not affect the measured intensity significantly. Hence we neglect this complicating factor in the rest of the paper.

The other sample was a thick (≃0.2 mm) Au film on which a carbon film with areal density 16.0 μg/cm^2 (700 Å thick) was placed, before the sample was introduced to the vacuum. Part of the Au was left uncovered. This uncovered part showed a single elastic peak, with no indication of contributions of C and O to the elastic peak. A separate Au film was sputter-cleaned using Ar^+ ions. However the obtained spectrum was identical before and after sputtering.

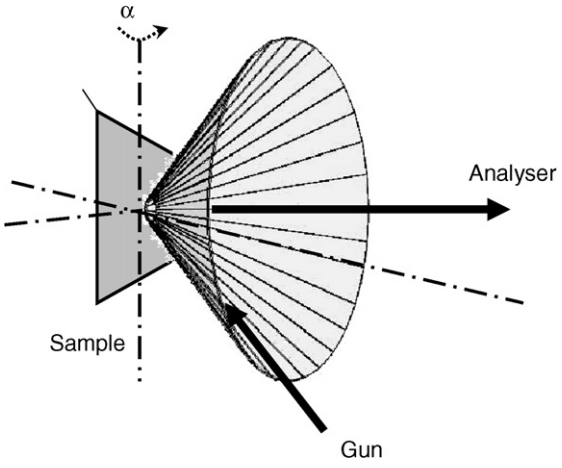

Fig. 1. A sketch of the experimental setup employed in this paper.

4. Results

In Fig. 2 we show the spectra of the elastic peak for a Au foil partly covered with a 700 Å thick C overlayer as a function of incoming beam energy (with the sample orientation $\alpha = 0$). These spectra were obtained in approximately half an hour using a beam current of 3 nA. There are two peaks visible, the one at lower energy loss is due to electrons scattering from Au atoms, the one at higher energy loss due to electrons scattered from C atoms. This interpretation can be verified by moving the beam to a part of the Au foil that is not covered by carbon. Then the peak at higher energy loss disappears. The separation of the peaks decreases with decreasing electron beam energy.

Clearly both peaks have a different full-width-at-half-maximum (FWHM). The width of the Au peak is attributed mainly to the experimental resolution. Values for σ of 0.20 eV are typically obtained for Au (corresponding to 0.47 eV FWHM). The carbon peak is an order of magnitude broader. This is attributed to the Doppler broadening term (Eq. (2)) which is much larger for carbon mainly

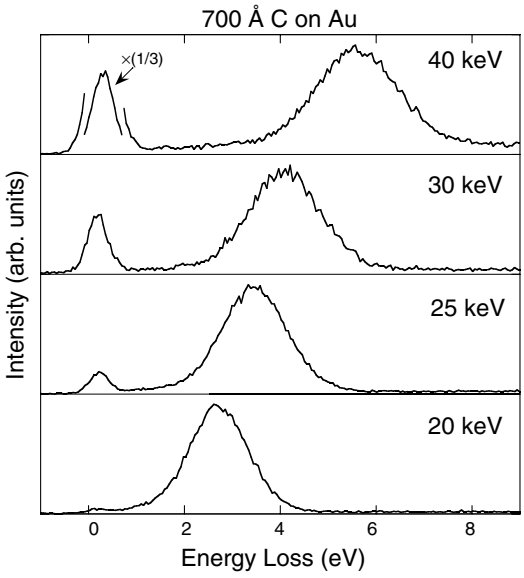

Fig. 2. The elastic peak spectra of a Au sample with a 700 Å C overlayer taken at incoming energies as indicated ($\alpha = 0$).

due to its smaller mass. For experiments using a 45° scattering angle, the peak shape of carbon is extensively discussed in [23].

The zero point of our spectrometer is hard to determine at a precision level better than 1 eV. The energy scale in the plots is hence adjusted in such a way that the Au peak is at an energy loss value corresponding to its recoil energy, as given in Table 1. The measured separation of the Au and C peak, however, can be compared with the ΔE_r as obtained from Table 1. This comparison is given in Table 2. The agreement is very good, even better than for the data taken at smaller momentum transfer using a scattering angle of 45° [23]. However, even under these conditions the observed peak separation seems systematically 1–2% smaller than the calculated one. This very small discrepancy could be a consequence of multiple scattering or an indication that the model, assuming that the electron scattered from a free nucleus rather than from one that is part of the crystal lattice, has its limitations.

For carbon, experimental determinations of the mean kinetic energy E_k range from 91 to 108 meV [23]. Using a value of 100 meV and Eq. (3) we obtain the theoretical estimate of the width (standard deviation) of the carbon peak. Agreement between the calculated widths and observed widths is excellent. Here we assume that all of the carbon width is due to Doppler broadening. A slightly different approach would be to assume that the observed width of Au is a good estimate of the experimental resolution. By subtracting this width from the carbon width in quadrature, we obtain then the intrinsic width σ_{int}: ($\sigma_{int} = \sqrt{\sigma_{obs}^2 - \sigma_{Au}^2}$). σ_{int} would then be about 5% smaller than σ_{obs}, and a good agreement with the prediction of Eq. (3) would be obtained by assuming $E_k \simeq 91$ meV.

It is clear from Fig. 2 that these measurements show a very strong dependence of relative peak height on beam energy. Similar strong effects are seen if we rotate the sample. This is illustrated in Fig. 3 for the case of 30 keV incoming electrons. Again the Au intensity decreases rapidly when the outgoing angle becomes more glancing, i.e. the measurement becomes more surface sensitive. The peak areas were determined from a fit using Gaussian peaks and often a Shirley-type background. The background is somewhat arbitrary, but the choice of background has in most cases only a small influence on the obtained peak area ratios. (It changes the value of I_o/I_s by less than 0.01.)

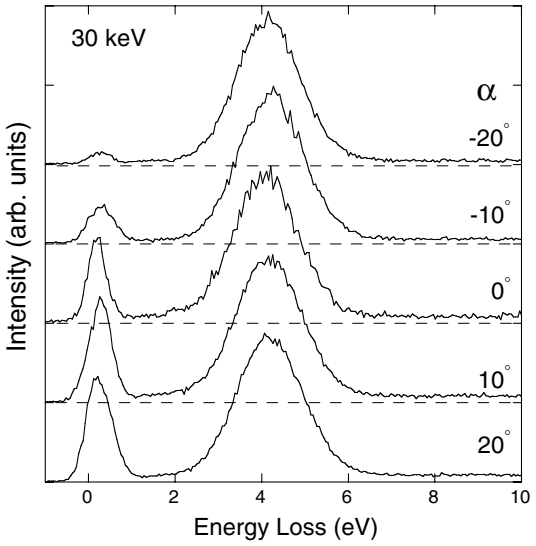

Fig. 3. The elastic peak spectra of 700 Å C on Au taken at 30 keV as a function of rotation angle α.

The observed ratios are shown in Table 3. Assuming the values of the IMFP and the scattering cross section given in Table 1 we can calculate the peak ratios using Eqs. (6) and (7). Using these values the calculated attenuation of the Au signal is too small. Using the IMFP of carbon and Au as fitting parameters we can obtain a good agreement between experiment and theory if we assume $\lambda_C = 320$ Å (instead of the TPP-2M value of 494 Å, but surprisingly close to the value of 315 Å as obtained from [19]) and $\lambda_{Au} = 150$ Å (instead of 192 Å). Both parameters influence the calculation in different ways. Roughly speaking, increasing the Au IMFP by x% increases the ratio I_{Au}/I_C by x% for all angles. Basically the thickness of the Au layer that effectively contributes to the Au elastic peak increases by x%. Decreasing the IMFP of C increases the attenuation effect of the overlayer, making the influence of the rotation on I_{Au}/I_C more pronounced.

In an earlier attempt to measure the IMFP of C using a scattering geometry with $\theta = 45°$ we also noticed that the mean free path of C at these energies should be much smaller than those obtained from TPP-2M. In that case, using 40 keV electrons (rather than 30 keV electrons), we found that value of 350 ± 50 Å (instead of the TPP-2M value of 637 Å) could describe the measurement satisfactorily [24].

Table 2
Observed and calculated Au–C peak splitting and Au and C peak width (σ) for a 700 Å thick C layer on Au, and for 4 Å thick Au layer on C

E_0 (keV)	ΔE_r obs. (eV)	ΔE_r calc. (eV)	σ obs. Au (eV)	σ obs. C (eV)	σ calc. C (eV)	Geom.
20	–	2.63	–	0.61	0.61	C on Au
25	3.24	3.29	0.20	0.68	0.68	C on Au
30	3.91	3.96	0.21	0.75	0.75	C on Au
40	5.30	5.35	0.22	0.86	0.87	C on Au
20	2.56	2.63	0.18	0.62	0.61	Au on C
25	3.23	3.29	0.19	0.69	0.68	Au on C
30	3.91	3.96	0.19	0.76	0.75	Au on C
40	5.25	5.35	0.21	0.86	0.87	Au on C

Table 3
Observed and calculated ratios of the Au and C peak areas at 30 keV for the indicated rotation angle α

α	θ_{in}	θ_{out}	I_{Au}/I_C observed	I_{Au}/I_C (I)	I_{Au}/I_C (II)
−20	48.3	65	0.02	0.28	0.02
−10	45.8	55	0.09	0.75	0.08
0	45.0	45	0.16	1.24	0.17
10	45.8	35	0.24	1.6	0.24
20	48.3	25	0.28	1.7	0.27

The observed values I_{Au}/I_C observed are compared to those obtained in calculation (I) using the TPP-2M values of the IMFP, and to those obtained from calculation (II), 'a best fit' obtained with $\lambda_C = 320$ Å and $\lambda_{Au} = 150$ Å.

Both the energy dependence and the angular dependence of the peak intensity ratio are very strong. This is because the carbon layer covering the Au substrate is thick (700 Å) and the trajectory length of electrons scattering from Au is at least 2000 Å ($2t/\sin 45°$), much larger than the IMFP. In spite of this Au is still clearly observed because of its huge elastic-scattering cross section.

How does the situation change if we put Au an a C substrate. In Fig. 4 we show the spectra of a carbon sample on which 4 Å of Au was deposited. Even for this small amount of Au, the Au signal dominates. Attenuation of the carbon signal in the Au layer is negligibly small. The carbon peak area is only a small fraction of the Au peak area because the Au cross section is so much larger. Now the angular dependence of the overlayer/substrate intensity ratio is very weak. This is somewhat obscured in the figure as the peak width of Au is somewhat dependent on the measurement geometry (presumably due to changes in the size of the beam hitting the surface, as seen by the analyzer). More accurate peak-area ratios were obtained from the fitting procedure. Changing the angle changes the effective thickness of the carbon film that contributes to the spectra, but attenuation of the C signal in the Au overlayer remains negligibly small.

In Fig. 5 we show the overlayer/substrate intensity ratio obtained from fits for both samples, as a function of energy and as a function of angle. Clearly both systems react differently to changes in the geometry or electron energy. The area ratio of the C-on-Au system is much more sensitive to these parameters than the ratio for the Au-on-C system.

In our interpretation of the C-on-Au spectra taken for different angles at 30 keV, we found that we obtained good agreement of the calculated intensity ratio with the observed one, if we divide the TPP-2M mean free path value of carbon by 1.54 and the value for Au by 1.28. In our calculation we assumed that the same scaling factors hold for the other energies. Using this assumption we can also calculate the intensity ratio for the spectra taken at different energies (and $\alpha = 0$). The theoretical values are shown in Fig. 5 as well. Agreement between experiment and theory,

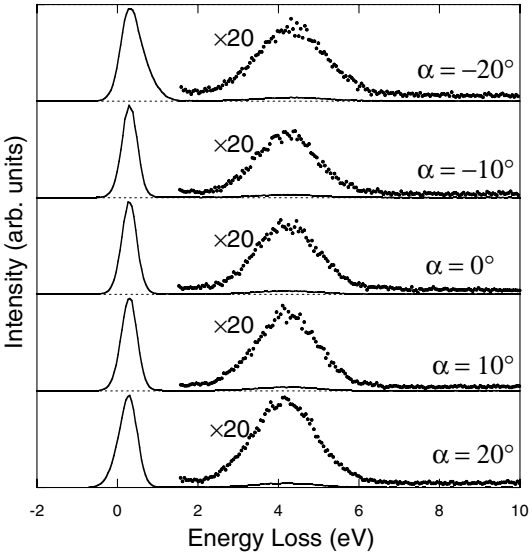

Fig. 4. The spectra of 4 Å Au on C obtained for sample orientations as indicated. In contrast to the C-on-Au system (Fig. 3) the changes of these spectra with orientation are minor.

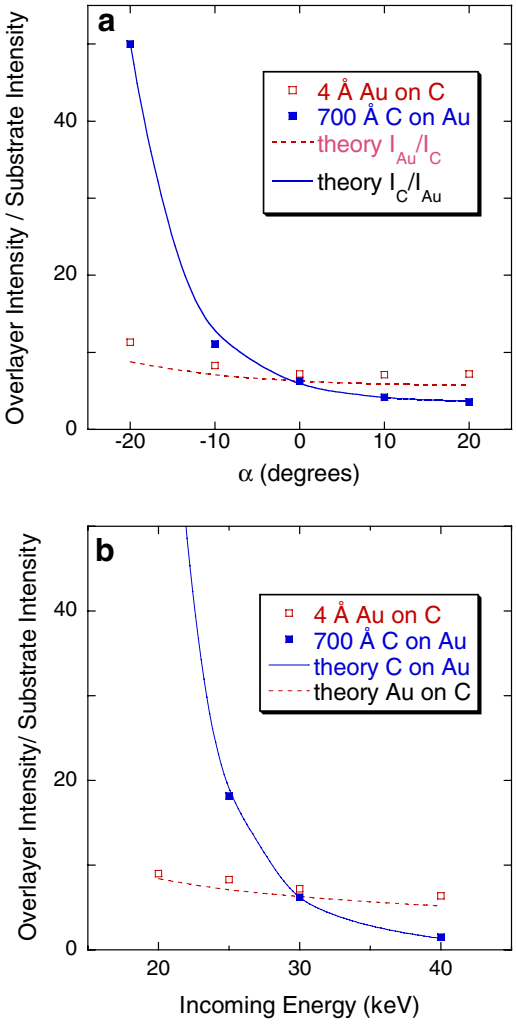

Fig. 5. The overlayer/substrate intensity ratio at different angles (a) and at different energies (b). For the 20 keV measurement the ratio is hard to determine, as the Au intensity is only 1–2% of the carbon area. The peak ratio can thus be anywhere between 50 and 100. A value of 90 was calculated.

using the adjusted mean free path values, is as good as can be expected.

Finally we increased the Au overlayer thickness to 9 Å. The broad carbon signal becomes weak, but is still distinct from the background. In Fig. 6 we show a 25 keV spectrum ($\alpha = 0$) from this sample, as well as the 25 keV sample of 700 Å C on Au. For both cases the substrate intensity is $5 \pm 1\%$ of the overlayer intensity and the information depth is thus the same as the overlayer thickness. Thus for these special cases an experimental determination of the overlayer depth was possible. Indeed it turns out that the information depth is much smaller than either the C or Au IMFP, for the case of a heavy overlayer on a light substrate. For the reverse case (light overlayer on heavy substrate) the information depth is much larger than either of the IMFP's.

It is interesting to note that the relative background component of the Au peak of Au buried under 700 Å of C is much larger than the background of the Au peak of 9 Å Au on C. In the first case the Au signal is severely attenuated by the C overlayer and as a consequence there is a large increase in intensity at small energy loss values. In the second case the Au layer at the surface is too thin for significant attenuation. Hence the latter Au peak has virtually no background. The background contains similar information on the sample morphology as the background of core level spectra measured by XPS, as described by Tougaard in e.g. [25].

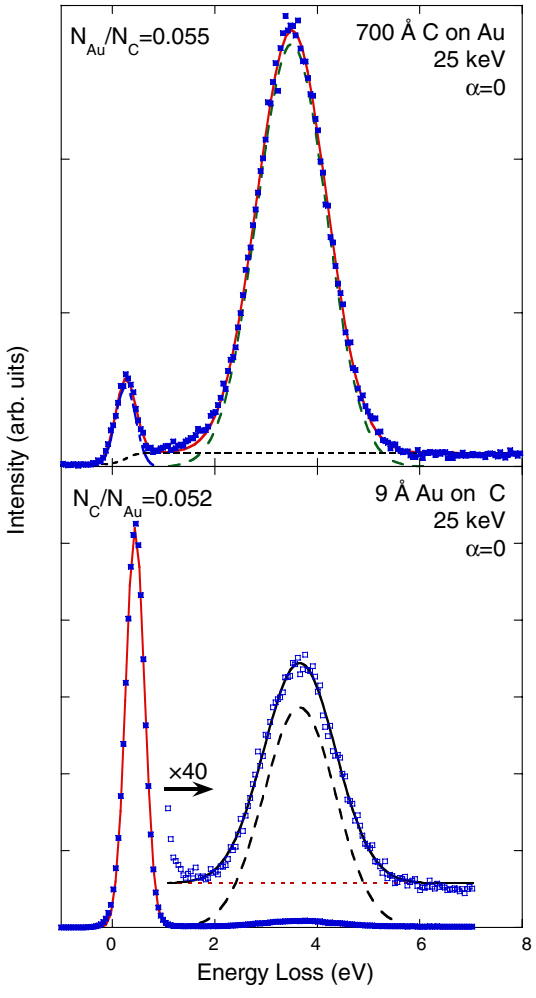

Fig. 6. Results of two experiments for which the substrate intensity is close to 5% of the overlayer intensity. The overlayer thickness corresponds in these cases to the probing depth. The top spectrum is for 700 Å C on Au, whereas the bottom spectrum is for 9 Å Au on C. Peak decomposition and shape of the background used in the area determination are shown as well.

5. Conclusion

High-resolution large-angle elastic-scattering experiments, in which the recoil energy is resolved, is a technique that provides new ways for testing our understanding of transport of energetic electrons in materials. We demonstrated here the potential of this technique by determining the ID in two-layer systems, as well as the IMFPs for Au and C. The predicted anomalous ID of these overlayer systems [14,15] was confirmed. The ID is reduced for a high Z overlayer on a low Z substrate, and increased for the reverse case.

Moreover, the splittings between the elastic peaks agree with the theory within 1–2%, whereas the width of the carbon peak could also be described well, based on earlier measurements of its mean kinetic energy. This level of agreement is a strong indication that the single scattering approximation, used to interpret these measurements, is quite valid under our experimental conditions. The internal consistency of these measurements, taken at different energies and angles is quite impressive, again supporting the single-scattering approach. The good quantitative consistency and interpretation using very simple single-scattering theory makes this technique a promising candidate for quantitative analysis of near-surface layers obtaining information of the composition in surface layers with thicknesses varying from 5–10 Å up to 1000 Å depending on the sample composition.

Acknowledgement

This work is made possible by a Grant of the Australian Research Council.

References

[1] G. Gergely, Progress in Surface Science 71 (2002) 31.
[2] A. Jablonski, Progress in Surface Science 74 (2003) 357.
[3] A. Jablonski, Progress in Surface Science 79 (2005) 3.
[4] L. Reimer, Scanning Electron Microscopy, Springer, Berlin, 1985.
[5] W.S.M. Werner, Surface and Interface Analysis 31 (2001) 141.
[6] H. Boersch, R. Wolter, H. Schoenebeck, Zeitschrift fur Physik 199 (1967) 124.
[7] D. Varga, K. Tökesi, Z. Berènyi, J. Tóth, L. Körvér, G. Gergely, A. Sulyok, Surface and Interface Analysis 31 (2001) 1019.
[8] M. Vos, Physical Review A 65 (2002) 12703.
[9] W.S.M. Werner, C. Tomastik, T. Cabela, G. Richter, H. Störi, Journal of Electron Spectroscopy and Related Phenomena 113 (2001) 127.

[10] D. Varga, K. Tokési, Z. Berényi, J. Tóth, L. Kövér, Surface and Interface Analysis 38 (2006) 544.
[11] G. Cooper, A. Hitchcock, C. Chatzidimitriou-Dreismann, M. Vos, Journal of Electron Spectroscopy and Related Phenomena, in press, doi:10.1016/j.elspec.2006.11.001.
[12] M.R. Went, M. Vos, Surface Science 600 (10) (2006) 2070.
[13] A. Jablonski, C. Powell, Surface Science 551 (2004) 106.
[14] L. Zommer, A. Jablonski, Journal of Electron Spectroscopy and Related Phenomena 150 (2006) 56.
[15] L. Zommer, Surface Science 600 (2006) 4735.
[16] M.P. Paoli, R.S. Holt, Journal of Physics C: Solid State Physics 21 (1988) 3633.
[17] M. Vos, C.A. Chatzidimitriou-Dreismann, T. Abdul-Redah, J. Mayers, Nuclear Instruments and Methods in Physical Research Section B 227 (2004) 233.
[18] S. Tanuma, C.J. Powell, D.R. Penn, Surface and Interface Analysis 20 (1993) 77.
[19] S. Tanuma, C.J. Powell, D.R. Penn, Surface and Interface Analysis 37 (2005) 1.
[20] F. Salvat, A. Jablonski, C.J. Powell, Computer Physics Communications 165 (2005) 157.
[21] V.M. Dwyer, Journal of Vacuum Science and Technology A: Vacuum Surfaces, and Films 12 (5) (1994) 2680.
[22] M. Vos, G.P. Cornish, E. Weigold, Review of Scientific Instruments 71 (2000) 3831.
[23] M. Vos, M.R. Went, Physical Review B 74 (2006) 205407.
[24] M. Went, M. Vos, R.G. Elliman, Journal of Electron Spectroscopy and Related Phenomena, in press, doi:10.1016/j.elspec.2006.11.041.
[25] S. Tougaard, Applied Surface Science 100 (1996) 1.